Pharmaceutical Sciences, 2020, 26(Suppl 1), S63-S77
doi:10.34172/PS.2020.57
https://ps.tbzmed.ac.ir/

Research Article

Molecular Docking of Novel 5-O-benzoylpinostrobin Derivatives as SARS-CoV-2 Main Protease Inhibitors

Mohammad Rizki Fadhil Pratama[1] Hadi Poerwono[2], Siswandono Siswodihardjo[2*]

[1] *Department of Pharmaceutical Sciences, Faculty of Pharmacy, Universitas Airlangga, Jl Dr Ir H Soekarno Mulyorejo, Surabaya, East Java, Indonesia.*
[2] *Department of Pharmaceutical Chemistry, Faculty of Pharmacy, Universitas Airlangga, Jl Dr Ir H Soekarno Mulyorejo, Surabaya, East Java, Indonesia.*

Article Info

Article History:
Received: 6 May 2020
Accepted: 13 July 2020
ePublished: 30 November 2020

Keywords:
-5-O-benzoylpinostrobin,
-Docking
-Remdesivir
-SARS-CoV-2
-Protease Inhibitors

Abstract

Background: COVID-19, a global pandemic caused by SARS-CoV-2 infection, has led researchers around the world to search for therapeutic agents for treatment of the disease. The main protease (M^{Pro}) of SARS-CoV-2 is one of the potential targets in the development of new drug compounds for the disease. Some known drugs such as chloroquine and remdesivir have been repurposed for treatment of COVID-19, although the the mechanism of action of these compounds is still unknown. In addition to these known drugs, new drug compounds such as 5-O-benzoylpinostrobin derivatives are also potentially used as SARS-CoV-2 M^{Pro} inhibitors. This study aims to determine the potential of 5-O-benzoylpinostrobin derivatives as SARS-CoV-2 M^{Pro} inhibitors, compared with several other compounds used in COVID-19 therapy.

Methods: *In silico* study was carried out by molecular docking of 5-O-benzoylpinostrobin derivatives using Autodock Vina on two SARS-CoV-2 M^{Pro} receptors with PDB IDs of 5R84 and 6LU7. The free energy of binding was calculated and the the interactions of each ligand were analyzed and compared with reference ligand.

Results: Three 5-O-benzoylpinostrobin derivatives each with fluoro, tertiary butyl, and trifluoromethyl substituents at 4-position of benzoyl group showed the lowest free energy of binding value and the highest similarity of ligand-receptor interactions with co-crystalized ligands. These three compounds even exhibited promising results in comparison with other reference ligands such as remdesivir and indinavir.

Conclusion: The results of this investigation anticipate that some 5-O-benzoylpinostrobin derivatives have the potential as SARS-CoV-2 M^{Pro} inhibitors.

Introduction

Since it first appeared at the end of 2019 in China, the Severe Acute Respiratory Syndrome Coronavirus 2 (SARS-CoV-2) virus has become a real threat to humanity throughout the world.[1] Until early May 2020, more than three million people worldwide were infected with a death toll of nearly two hundred fifty-thousand. Aside from its rapid spread, another factor that causes the virus to continue to be very deadly is the possibility of mutations, which make it difficult to develop vaccines and antiviral drugs to treat them.[2,3]

One of the most rational strategies to overcome this is by drug repurposing of drugs that are currently used. Besides being able to shorten the time needed for testing, it can also reduce the costs required for developmental process.[4] However, the virus that causes a disease called COVID-19 reportedly did not respond well to pharmacotherapy with several drugs that are currently being tested. Recent studies reported by Wang et al. demonstrated that remdesivir which had been predicted to be effective in treating COVID-19 did not show a significant clinical benefit.[5] Several other clinical studies related to remdesivir are still ongoing and are expected to provide more promising results.[6] In addition to remdesivir, other drugs that are also being tested for COVID-19 treatment are favipiravir, chloroquine, and hydroxychloroquine which also show promising results.[7,8] Testing of these drugs also continues while exploration to find other potential compounds.

Amid limitations of drug testing for COVID-19 related to the time and cost required for testing both preclinically and clinically, screening of potential compounds are carried outvia in silico approaches is the most rational choice for COVID-19 drug discovery.[9,10] Some studies are focused on investigations on several known antivirals such as remdesivir and lopinavir,[11,12] while the other researches are conducted on secondary metabolites from various medicinal plants as candidates for pharmacotherapy of COVID-19.[13-16] Some secondary metabolites from medicinal plants such as andrographolide group from *Andrographis paniculata* show promising results as SARS-CoV-2 main protease inhibitors.[17]

*Corresponding Author: Siswandono Siswodihardjo, E-mail: prof.sis@ff.unair.ac.id

SARS-CoV-2 main protease (M^{pro}, also known as $3CL^{pro}$) is one of the attractive targets in COVID-19 therapy besides Angiotensin-converting enzyme II (ACE2) and RNA-dependent RNA polymerase (RdRp) because of its crucial role in processing the polyproteins that are translated from the viral RNA.[18,19] Compared to ACE 2 and RdRp, inhibition of SARS-CoV-2 M^{Pro} shows the potential for less significant side effects and higher efficacy, making it as the most attractive target in developing COVID-19 drugs.[20] Several new compounds have been developed specifically as SARS-CoV-2 M^{Pro} inhibitors, as did Jin et al. by developing N3 inhibitors with quite promising potential.[21] Moreover, several other types of SARS-CoV-2 M^{Pro} inhibitors with smaller size such as ethanamide derivatives were also identified.[22,23] Exploration of SARS-CoV-2 M^{Pro} inhibitors with computational methods for various compounds both from natural metabolites and synthetic compounds was intensively carried out to find compounds with optimum potential and minimum side effects.[24]

One of the compounds that can be considered in the development of inhibitors is 5-O-benzoylpinostrobin (a benzoyl derivative from pinostrobin) a flavanone that can be isolated from the *Boesenbergia pandurata* rhizome in large enough quantities. Pinostrobin is known to have antiviral activity against several types of viruses such as Dengue and Herpes Simplex virus, although the antiviral activity of this compound has not been studied on the Coronaviridae family yet.[25] Pinostrobin is also reported to have inhibitory activity on protease inhibitor of the virus although it is relatively weak,[26] so it is anticipated that its derivatives may have the potential for viral protease inhibitor activity. Furthermore, 5-O-benzoylpinostrobin compound is designed as a HER2 antagonist and evaluated for treatment of HER2-positive breast cancer and is currently in the stage of synthesis and preclinical testing.[27] These type of compounds which also have the potential as L858R/T790M/V948R mutant EGFR inhibitors also have ADMET properties that support to be developed as drug compounds, with the class IV toxicity category.[28,29]

The purpose of this study is to determine the potential of 5-O-benzoylpinostrobin derivatives as SARS-CoV-2 M^{Pro} inhibitors, compared with several other compounds used in the development of COVID-19 therapy. *In silico* research for the 5-O-benzoylpinostrobin derivatives was carried out using the molecular docking method, using seven drug compounds currently developed in COVID-19 therapy as reference ligands. A total of 14 test ligands consisting of pinostrobin and 5-O-benzoylpinostrobin derivatives were tested against the SARS-CoV-2 M^{Pro} receptor which binds to the inhibitor. Evaluation of docking results are carried out based on two main parameters consisting of the free energy of binding (ΔG) and the similarity of ligand-receptor interactions, to be compared with the co-crystal ligand of the receptor and the reference ligand. Test ligands with the lowest ΔG values and the highest % similarity of ligand-receptor interactions of co-crystal ligands were subsequently determined as test ligands with the highest potential as SARS-CoV-2 M^{Pro} inhibitors.

Materials and Methods

Materials

The hardware used was the ASUS A46CB series Ultrabook with an Intel™ Core i5-3337U@1.8 GHz and Windows 7 Ultimate 64-bit SP-1 operating system. The software used were HyperChem 7.5 for molecular modeling and energy minimization, OpenBabel 2.4.1 for ligand and receptor format conversion, AutoDockTools 1.5.6 for docking protocol configuration, Autodock Vina 1.1.2 for the docking process, PyMOL 2.3.1 for docking protocol validation, UCSF Chimera 1.13.1 for the preparation of docking results, and Discovery Studio Visualizer 19.1.0.18287 for visualization and observation of docking results.[30-33] Information on three-dimensional structures of receptor obtained from the website of Protein Data Bank http://www.rscb.org.

Ligands preparation

The test ligands were consisted of pinostrobin and 13 compounds of 5-O-benzoylpinostrobin derivatives with various substituent on the benzoyl moiety, while the reference ligand was a drug compound that was being tested in COVID-19 therapy including chloroquine, hydroxychloroquine, favipiravir, indinavir, lopinavir, nelfinavir, and remdesivir, as shown in Table 1. The two-dimensional structure was sketched using HyperChem 7.5. with geometry optimization ab initio and basis set of 6-31G*. Optimization was done by the Polak-Ribiere algorithm and RMS Gradient of 0.1 kcal/mol. The format of optimized structure were converted from *.hin to *.pdb using Open Babel 2.4.1. Then the charge of the ligands then are given the charge and set torque by default using AutoDockTools 1.5.6.[34]

Receptors preparation

The receptors used are SARS-CoV-2 M^{Pro} (PDB ID 5R84 and 6LU7) each with a co-crystal ligand of 2-cyclohexyl-~{N}-pyridin-3-yl-ethanamide and N-[(5-methylisoxazol-3-yl)carbonyl]alanyl-l-valyl-N~1~-((1R,2Z)-4-(benzyloxy)-4-oxo-1-{[(3R)-2-oxopyrrolidin-3-yl]methyl}but-2-enyl)-l-leucinamide, respectively.[21] Both receptors contain the main protease monomer from SARS-CoV-2 with different orientations due to different binding co-crystal ligands. The resolution of the two receptor crystal structures is in the range of 1.83 to 2.16 Å. Information on three-dimensional structures of receptor proteins was obtained from the website of Protein Data Bank (http://www.rscb.org).

Validation of docking protocol

Before the docking process for test ligands, initially the validation of the docking protocol is conducted. The redocking process is performed using co-crystal ligands of each receptor.[35] Both co-crystal ligands from the proteins (PDB IDs: 5R84 and 6LU7) were extracted, added the

Table 1. The two-dimensional structure of all test and reference ligands

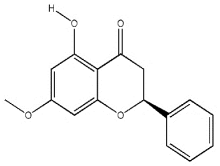 Pinostrobin	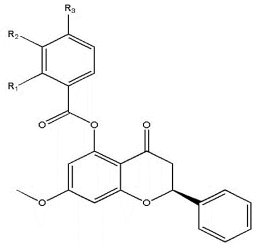 5-O-Benzoylpinostrobin
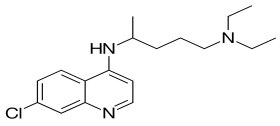 Chloroquine	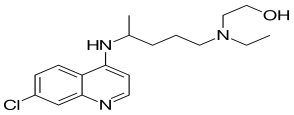 Hydroxychloroquine
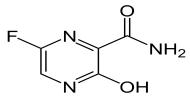 Favipiravir	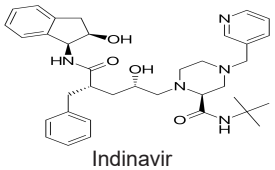 Indinavir
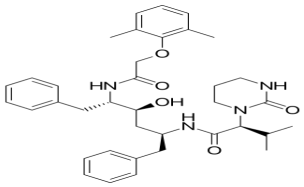 Lopinavir	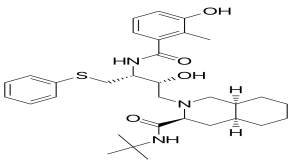 Nelfinavir
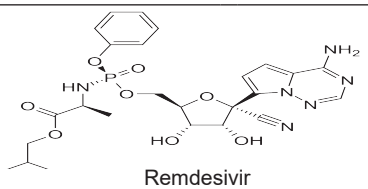 Remdesivir	

Compounds Name	Code	Functional group		
		R_1	R_2	R_3
Pinostrobin	P	-	-	-
5-O-Benzoylpinostrobin	BP	H	H	H
2-Chloro-5-O-benzoylpinostrobin	2Cl	Cl	H	H
3-Chloro-5-O-benzoylpinostrobin	3Cl	H	Cl	H
4-Chloro-5-O-benzoylpinostrobin	4Cl	H	H	Cl
2,4-Dichloro-5-O-benzoylpinostrobin	24Cl	Cl	H	Cl
3,4-Dichloro-5-O-benzoylpinostrobin	34Cl	H	Cl	Cl
4-Bromo-5-O-benzoylpinostrobin	4Br	H	H	Br
4-Fluoro-5-O-benzoylpinostrobin	4F	H	H	F
4-Nitro-5-O-benzoylpinostrobin	4NO	H	H	NO_2
4-Methyl-5-O-benzoylpinostrobin	4C	H	H	CH_3
4-Methoxy-5-O-benzoylpinostrobin	4OC	H	H	OCH_3
4-Trifluoromethyl-5-O-benzoylpinostrobin	4CF	H	H	CF
4-t-Butyl-5-O-benzoylpinostrobin	4TB	H	H	$(CH_3)_3$
Chloroquine	CQ	-	-	-
Hydroxychloroquine	HCQ	-	-	-
Favipiravir	FVP	-	-	-
Indinavir	IND	-	-	-
Lopinavir	LPN	-	-	-
Nelfinavir	NFN	-	-	-
Remdesivir	RMD	-	-	-

polar hydrogen group, given the charge, torque, and the rotational bonds were adjusted, then stored in the *.pdbqt format. The co-crystal ligand was then redocked at the grid box position and size predetermined from the orientation result.[36] The orientation is done in such a way as to obtain the smallest size grid box that can contain the whole ligand.[37] The parameters observed in the validation process are the root-mean-square deviation (RMSD) of co-crystal ligand at the selected binding site using PyMOL 2.3.1. The docking protocol is valid if an RMSD value of no more than 2 Å is obtained.[38]

Molecular docking

Docking for all tests and reference ligands performed in the same way as the validation process with similar sizes and positions of the grid box. Running for the docking process is done with Autodock Vina 1.1.2. The main parameters used in the docking process with Autodock Vina were the ΔG and the similarity of ligand-receptor interactions.[39] The similarity of ligand-receptor interactions is obtained by multiplying the percentage of amino acid similarity with the percentage of similarity in the type of interaction that occurs. The higher ligand-receptor interaction similarity indicates a higher probability that the ligand test will have a similar mechanism of action compared to co-crystal ligands.[40] The docking process is replicated five times and the mean value for ΔG is used, while the standard deviation limit values should not be more than 0.2 kcal/mol. Ligand pose with the lowest ΔG is then stored in *.pdb format using Chimera 1.13.1. Two dimensional analyses of docking resultswere performed using Discovery Studio Visualizer 19.1.0.

Results

Validation of docking protocol

The RMSD value obtained from the redocking process for the 5R84 and 6LU7 receptors was 0.802 Å and 1.981 Å, respectively. This indicated that the docking protocol for both receptors was valid for docking purposes. The visualization of ligands overlays from redocking with co-crystal ligands from crystallographic results is presented in Figure 1. There are 14 and 25 amino acids, respectively, that interact at the 5R84 and 6LU7 receptors. The number of amino acids in the binding site of 6LU7 receptor are greater than those for 5R84 due to the larger size of the corresponding co-crystal ligand and the dimension of the grid box. Of these, there are 14 amino acids that both interact with co-crystal ligands in both receptors. However, only nine amino acids have the same type of interactions specially van der Waals interactions. In conclusion, the redocking process shows that the docking protocol on the two receptors can be used for the docking process. The parameters observed in the validation process are ΔG and amino acid interactions, as well as the size and coordinates of the grid box, as shown in Table 2.

Molecular docking

The docking of all test and reference ligands showed exciting results with some consistent patterns in both the 5R84 and 6LU7 receptors. First, there is a striking difference in the ranking order of the ΔG values of all test ligands in the two receptors, as presented in Tables 3 and 4. Some ligands have very low ΔG values (a difference of more than 1.0 kcal/mol compared to co-crystal ligand) at the 5R84 receptor but are high enough at the 6LU7 receptor, as shown by 5-O-benzoylpinostrobin and 4-methyl-5-O-benzoylpinostrobin, including pinostrobin itself. This shows that the ligands have interaction patterns that are more suited to the orientation of the 5R84 receptor that binds to co-crystal ligands that are not too large in size. On the other hand, some ligands consistently have a smaller ΔG value than co-crystal ligands on both receptors, as indicated by 4-fluoro-5-O-benzoylpinostrobin, 4-t-butyl-5-O-benzoylpinostrobin, and 4-trifluoromethyl-5-O-benzoylpinostrobin. Considering these conditions, only the three ligands are predicted to be potential inhibitors for both the 5R84 and 6LU7 receptors. The 3,4-dichloro-5-O-benzoylpinostrobin also shows a similar condition, but the difference in the value of ΔG with the co-crystal ligand on the 6LU7 receptor is very small (0.02 kcal/mol).

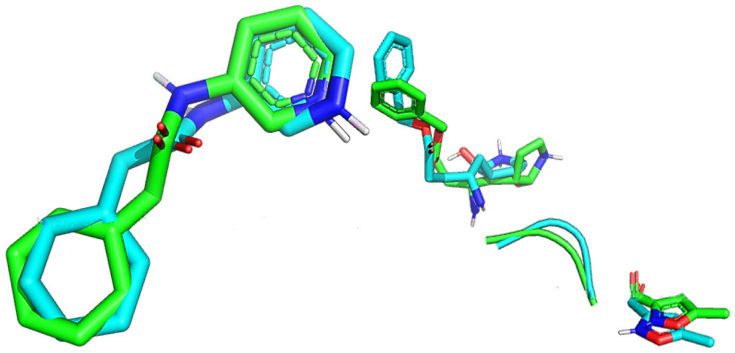

Figure 1. Overlays of redocking ligands (blue) with co-crystal ligands from X-crystallography data (green) at receptors (A) 5R84 with RMSD 0.802 Å and (B) 6LU7 with RMSD 1.981 Å

Second, from the standpoint of interaction similarity, there is a difference in the % similarity of ligand-receptor interactions in the two receptors. For the 5R84 receptors, the similarity is in the range of 24.49% to 50%, while at 6LU7 receptors are in the range of 11.2% to 32%. This difference shows that the interaction of the test ligand is more similar to the co-crystal ligand of the 5R84 receptor than the 6LU7 receptor. This is predicted due to differences in the type and size of the two co-crystal ligands, where 2-cyclohexyl-~{N}-pyridin-3-yl-ethanamide has dimensions that are closer to the average dimensions of the test ligand than N-[(5-methylisoxazol-3-yl)carbonyl] alanyl-l-valyl-N~1~-((1R,2Z)-4-(benzyloxy)-4-oxo-1-{[(3R)-2-oxopyrrolidin-3-yl]methyl}but-2-enyl)-l-leucinamide. What is interesting is that the three ligands that have the lowest ΔG value compared to co-crystal ligands also have a fairly high % similarity in the range of 33.16% to 50% at the 5R84 receptor and 18.24% to 32% at the 6LU7 receptor. These points reinforce the prediction that the three compounds are 5-O-benzoylpinostrobin derivatives which have the most potential as SARS-CoV-2 M^{Pro} inhibitors. Also, all three test ligands have relatively similar binding motives for both receptors, as can be seen visually in Figures 2 and 3.

Compared to all reference ligands, remdesivir and indinavir always have lower ΔG values than each co-crystal ligand, as presented in Tables 5 and 6. Also, the ligand-receptor similarity compared to the two co-crystal ligands

Table 2. Results of the validation process

Parameters		Values
PDB ID	5R84	6LU7
Co-crystal ligand	2-cyclohexyl-~{N}-pyridin-3-yl-ethanamide	N-[(5-methylisoxazol-3-yl)carbonyl]alanyl-l-valyl-N~1~-((1R,2Z)-4-(benzyloxy)-4-oxo-1-{[(3R)-2-oxo-pyrrolidin-3-yl]methyl}but-2-enyl)-l-leucinamide
Grid box size (Å)	28 x 14 x 24	40 x 54 x 40
Grid box position	x: 9.812 y: -0.257 z: 20.406	x: -9.732 y: 11.403 z: 68.483
RMSD (Å)	0.802	1.981
ΔG (kcal/mol)	-6.4 ± 0.0	-8.12 ± 0.04
Amino acid residues	-	24-Thr[a]
	-	25-Thr[a]
	-	26-Thr[a]
	41-His[b]	41-His[b]
	49-Met[b]	49-Met[b]
	-	54-Tyr[a]
	140-Phe[a]	140-Phe[c]
	141-Leu[a]	141-Leu[d]
	142-Asn[a]	142-Asn[a]
	-	143-Gly[c]
	144-Ser[a]	144-Ser[a]
	145-Cys[a]	145-Cys[a]
	163-His[c]	163-His[c]
	164-His[c]	164-His[c]
	165-Met[b]	165-Met[c]
	166-Glu[a]	166-Glu[c]
	-	167-Leu[b]
	-	168-Pro[b]
	-	172-His[c]
	187-Asp[a]	187-Asp[a]
	188-Arg[a]	188-Arg[a]
	189-Gln[a]	189-Gln[c]
	-	190-Thr[c]
	-	191-Ala[b]
	-	192-Gln[a]

[a]Van der Waals interaction; [b]Alkyl/Pi-alkyl interaction; [c]Hydrogen bond; [d]Pi-Pi T-shaped/Pi-Pi Stacked/Amide-Pi stacked

Table 3. Results of the docking of all test ligands at the binding site of 5R84 receptor

Ligand	P	BP	2Cl	3Cl	4Cl	24Cl	34Cl	4Br	4F	4NO	4C	4OC	4CF	4TB
ΔG (kcal/mol)	-6.98 ±0.04	-7.50 ±0.00	-7.28 ±0.04	-7.30 ±0.00	-7.50 ±0.00	-7.58 ±0.04	-7.44 ±0.05	-7.28 ±0.04	-7.94 ±0.05	-7.40 ±0.00	-7.66 ±0.05	-7.58 ±0.04	-7.38 ±0.04	-7.30 ±0.00
Amino acid residues	-	25-Thr[a]	25-Thr[e]	25-Thr[a]	25-Thr[a]	25-Thr[a]	-	25-Thr[e]	25-Thr[a]	25-Thr[e]	25-Thr[a]	25-Thr[a]	25-Thr[e]	-
	-	26-Thr[a]	26-Thr[a]	26-Thr[a]	26-Thr[a]	26-Thr[a]	-	-	-	26-Thr[a]	26-Thr[a]	-	26-Thr[a]	-
	41-His[d]	41-His[d]	41-His[h]	41-His[d]	41-His[d]	41-His[h]	41-His[d]	41-His[d]	41-His[d]	41-His[d]	41-His[d]	41-His[d]	41-His[d]	41-His[a]
	-	-	-	-	44-Cys[b]	44-Cys[c]	-	44-Cys[c]	-	44-Cys[a]	44-Cys[b]	44-Cys[a]	44-Cys[b]	-
	49-Met[b]	49-Met[b]	49-Met[b]	49-Met[f]	49-Met[b]	49-Met[b]	49-Met[b]	49-Met[g]	49-Met[b]	49-Met[b]	49-Met[b]	49-Met[g]	49-Met[f]	49-Met[b]
	52-Pro[a]	-	-	52-Pro[b]	52-Pro[b]	52-Pro[b]	52-Pro[a]	52-Pro[b]	52-Pro[a]	52-Pro[a]	52-Pro[b]	52-Pro[a]	52-Pro[b]	52-Pro[a]
	54-Tyr[a]	54-Tyr[a]	-	54-Tyr[a]	54-Tyr[c]	54-Tyr[a]	54-Tyr[a]	54-Tyr[c]	54-Tyr[c]	54-Tyr[c]	54-Tyr[a]	54-Tyr[c]	54-Tyr[c]	54-Tyr[a]
	140-Phe[c]	140-Phe[a]	140-Phe[a]	140-Phe[a]	140-Phe[c]	140-Phe[a]	140-Phe[c]	140-Phe[a]	140-Phe[a]	140-Phe[c]	140-Phe[c]	140-Phe[a]	140-Phe[c]	140-Phe[c]
	141-Leu[a]	141-Leu[a]	141-Leu[a]	141-Leu[c]	141-Leu[a]	141-Leu[c]	141-Leu[a]	141-Leu[c]	141-Leu[c]	141-Leu[a]	141-Leu[a]	141-Leu[c]	141-Leu[a]	141-Leu[b]
	142-Asn[c]	142-Asn[a]	142-Asn[a]	142-Asn[a]	142-Asn[a]	142-Asn[a]	142-Asn[a]	142-Asn[a]	142-Asn[a]	142-Asna	142-Asna	142-Asna	142-Asn[a]	142-Asn[a]
	-	143-Gly[a]	143-Gly[a]	143-Gly[a]	143-Gly[a]	143-Gly[a]	-	143-Gly[a]	143-Gly[a]	143-Gly[a]	143-Gly[a]	143-Gly[a]	143-Gly[a]	-
	144-Ser[a]	144-Ser[a]	-	144-Ser[a]	144-Ser[a]	144-Ser[a]	144-Ser[a]	144-Ser[a]	144-Ser[a]	-	144-Ser[a]	144-Ser[a]	144-Ser[a]	144-Ser[a]
	145-Cys[a]	145-Cys[b]	145-Cys[b]	145-Cys[b]	145-Cys[b]	145-Cys[b]	145-Cys[a]	145-Cys[b]	145-Cys[b]	145-Cys[b]	145-Cys[b]	145-Cys[c]	145-Cys[b]	145-Cys[a]
	163-His[a]	163-His[a]	163-Hisa	163-His[a]	163-His[a]	163-His[a]	163-His[a]	163-His[a]	163-His[a]	163-His[a]	163-His[a]	163-His[a]	163-His[a]	163-His[a]
	164-His[a]	164-His[a]	164-His[f]	164-His[a]	-	164-His[f]	164-His[a]	-	164-His[a]	-	-	164-His[a]	-	164-His[a]
	165-Met[a]	165-Met[b]	165-Met[b]	165-Met[b]	165-Met[a]	165-Met[b]	165-Met[a]	165-Met[a]	165-Met[b]	165-Met[a]	165-Met[a]	165-Met[b]	165-Met[b]	165-Meta
	166-Glu[c]	166-Glu[c]	166-Glu[c]	166-Glu[c]	166-Glu[c]	166-Glu[c]	166-Glu[c]	166-Glu[c]	166-Gluc	166-Glu[a]	166-Glu[c]	166-Glu[c]	166-Glu[c]	166-Glu[a]
	-	-	-	-	-	-	168-Prob	-	-	-	-	-	-	-
	187-Asp[a]	187-Asp[a]	-	187-Asp[a]	-	-	187-Asp[a]	-	187-Asp[f]	187-Asp[a]	187-Asp[a]	187-Asp[a]	187-Asp[f]	187-Asp[a]
	188-Arg[d]	188-Arg[d]	188-Arg[a]	188-Arg[d]	188-Arg[a]	188-Arg[a]	188-Arg[d]	188-Arg[a]	188-Arg[d]	188-Arg[c]	188-Arg[a]	188-Arg[d]	188-Arg[c]	188-Arg[d]
	189-Gln[a]	189-Gln[c]	189-Gln[c]	189-Gln[c]	189-Gln[a]	189-Gln[a]	189-Gln[a]	189-Gln[c]	189-Gln[c]	189-Gln[a]	189-Glna	189-Glnc	189-Gln[a]	189-Gln[a]
The similarity of amino acids with co-crystal ligand (%)	100	100	85.71	100	85.71	92.86	100	85.71	100	85.71	92.86	100	92.86	100
The similarity in the type of interaction with co-crystal ligand (%)	42.86	50	42.86	35.71	42.86	50	50	28.57	35.71	42.86	50	35.71	35.71	50
The similarity of ligand-receptor interaction* (%)	42.86	50	36.73	35.71	36.73	46.43	50	24.49	35.71	36.73	46.43	35.71	33.16	50

[a]Van der Waals interaction; [b]Alkyl/Pi-alkyl interaction; [c]Hydrogen bond; [d]Pi-Pi T-shaped/Pi-Pi Stacked/Amide-Pi stacked; [e]Pi-sigma interaction; [f]Halogen; [g]Pi-Sulfur; [h]Unfavorable Bump/Donor-donor; *Similarity of amino acids x similarity in type of interaction

Table 4. Results of the docking of all test ligands at the binding site of 6LU7 receptor

Ligand	P	BP	2Cl	3Cl	4Cl	24Cl	34Cl	4Br	4F	4NO	4C	4OC	4CF	4TB
ΔG (kcal/mol)	-6.90 ±0.10	-7.94 ±0.09	-8.20 ±0.07	-8.24 ±0.05	-7.80 ±0.00	-8.00 ±0.07	-8.14 ±0.09	-7.72 ±0.08	-7.80 ±0.00	-8.24 ±0.05	-7.82 ±0.04	-7.98 ±0.08	-8.36 ±0.05	-8.44 ±0.05
Amino acid residues	-	-	-	-	-	-	-	-	-	24-Thr[a]	-	-	-	24-Thr[a]
	-	25-Thr[a]	25-Thr[a]	25-Thr[a]	25-Thr[a]	25-Thr[a]	25-Thr[a]	25-Thr[a]	25-Thr[a]	25-Thr[a]	25-Thr[a]	25-Thr[a]	25-Thr[a]	25-Thr[a]
	-	26-Thr[a]	26-Thr[a]	26-Thr[a]	26-Thr[a]	26-Thr[a]	26-Thr[a]	-	26-Thr[a]	26-Thr[a]	26-Thr[a]	26-Thr[a]	26-Thr[a]	26-Thr[a]
	-	27-Leu[b]	27-Leu[b]	27-Leu[b]	27-Leu[b]	27-Leu[b]	27-Leu[b]	-	27-Leu[b]	27-Leu[a]	27-Leub	27-Leu[b]	-	-
	41-His[a]	41-His[d]	41-His[d]	41-His[a]	41-His[a]	41-His[d]	41-His[d]	41-His[a]	41-His[d]	41-His[a]	41-His[d]	41-His[d]	41-His[d]	41-His[a]
	-	-	-	-	-	-	-	46-Ser[a]	-	-	-	-	-	-
	49-Met[b]	49-Met[c]	49-Met[b]	49-Met[f]	49-Met[c]	49-Met[b]	49-Met[b]	49-Met[a]	49-Met[c]	49-Met[a]	49-Met[c]	49-Met[c]	49-Met[e]	49-Met[a]
	-	52-Pro[a]	-	-	-	-	-	-	-	-	-	-	-	-
	54-Tyr[a]	54-Tyr[a]	-	54-Tyr[c]	54-Tyr[c]	-	54-Tyr[a]	-	54-Tyr[c]	-	54-Tyr[c]	54-Tyr[a]	54-Tyr[c]	-
	140-Phe[c]	-	140-Phe[a]	-	-	-	-	140-Phe[a]	-	140-Phe[a]	-	-	140-Phe[c]	140-Phe[c]
	141-Leu[a]	-	141-Leu[a]	-	-	-	-	141-Leu[a]	-	141-Leu[a]	-	-	141-Leu[a]	141-Leu[a]
	142-Asn[a]	-	142-Asn[c]	-	-	-	-	142-Asn[a]	-	142-Asn[a]	-	-	142-Asn[a]	142-Asn[a]
	143-Gly[a]	143-Gly[a]	143-Gly[a]	143-Gly[a]	143-Gly[a]	143-Gly[a]	143-Gly[a]	143-Gly[c]	143-Gly[a]	143-Gly[c]	143-Gly[a]	143-Gly[a]	143-Gly[c]	143-Gly[c]
	144-Ser[a]	144-Ser[a]	144-Sera	144-Sera	144-Sera	144-Sera	144-Sera	144-Serc	144-Sera	144-Serc	144-Sera	144-Sera	144-Sera	144-Ser[c]
	145-Cys[f]	145-Cys[b]	145-Cys[c]	145-Cys[b]	145-Cys[b]	145-Cys[b]	145-Cys[b]	145-Cys[c]	145-Cys[b]	145-Cys[f]	145-Cys[b]	145-Cys[b]	145-Cys[b]	145-Cys[c]
	163-His[c]	-	-	-	-	-	-	163-His[d]	-	-	-	-	163-His[a]	163-His[c]
	164-His[a]	164-His[a]	164-His[a]	164-His[a]	164-His[a]	164-Hisa	164-Hisa	164-His[a]	164-His[a]	164-His[a]	164-His[a]	164-His[a]	164-His[a]	164-His[a]
	165-Met[a]	165-Met[f]	165-Met[f]	165-Met[f]	165-Met[b]	165-Met[b]	165-Met[b]	165-Met[b]	165-Met[f]	165-Met[f]	165-Met[b]	165-Met[b]	165-Met[b]	165-Met[b]
	166-Glu[c]	166-Glu[a]	166-Glu[a]	166-Glu[a]	166-Glu[a]	166-Glu[a]	166-Glu[a]	166-Glu[a]	166-Glu[a]	166-Glu[c]	166-Glu[a]	166-Glu[a]	166-Glu[a]	166-Glu[c]
	-	167-Leu[a]	-	167-Leu[a]	-	-	-	-	167-Leu[a]	-	-	-	-	-
	-	168-Pro[b]	-	168-Pro[b]	-	168-Pro[b]	168-Pro[b]	-	168-Pro[a]	-	-	-	-	-
	172-His[a]	-	-	-	-	-	-	-	-	-	-	-	172-His[a]	172-His[a]
	187-Asp[a]	187-Asp[a]	-	187-Asp[a]	187-Asp[a]	187-Asp[a]	187-Asp[a]	-	187-Asp[a]	-	187-Asp[a]	187-Asp[a]	187-Asp[e]	-
	188-Arg[a]	188-Arg[a]	188-Arg[a]	188-Arg[a]	188-Arg[a]	188-Arg[a]	188-Arg[a]	188-Arg[a]	188-Arg[a]	188-Arg[a]	188-Arg[a]	188-Arga	188-Arg[e]	188-Arg[a]
	189-Gln[g]	189-Gln[g]	189-Gln[a]	189-Gln[g]	189-Gln[g]	189-Gln[g]	189-Gln[g]	189-Gln[a]	189-Gln[g]	189-Gln[a]	189-Gln[g]	189-Gln[g]	189-Gln[c]	189-Gln[a]
	-	190-Thr[a]	190-Thr[a]	190-Thr[a]	-	190-Thr[a]	190-Thr[a]	190-Thr[a]	190-Thr[e]	190-Thr[a]	-	190-Thr[a]	-	190-Thr[a]
	-	-	-	-	-	191-Ala[a]	191-Ala[a]	-	191-Ala[a]	-	-	191-Ala[a]	-	-
	-	192-Gln[a]	-	192-Gln[a]	-	192-Gln[a]	192-Gln[a]	192-Gln[a]	192-Gln[a]	-	-	-	-	192-Gln[a]

Table 4. Continued.

The similarity of amino acids with co-crystal ligand (%)	68	72	64	72	56	68	72	68	76	68	56	64	76	80
The similarity in the type of interaction with co-crystal ligand (%)	36	32	20	32	20	32	36	20	24	28	24	24	28	40
The similarity of ligand-receptor interaction* (%)	24.48	23.04	12.8	23.04	11.2	21.76	25.92	13.6	18.24	19.04	13.44	15.36	21.28	32

[a]Van der Waals interaction; [b]Alkyl/Pi-alkyl interaction; [c]Hydrogen bond; [d]Pi-Pi T-shaped/Pi-Pi Stacked/Amide-Pi stacked; [e]Halogen; [f]Pi-Sulfur; [g]Pi-Cation/Anion; *Similarity of amino acids x similarity in type of interaction

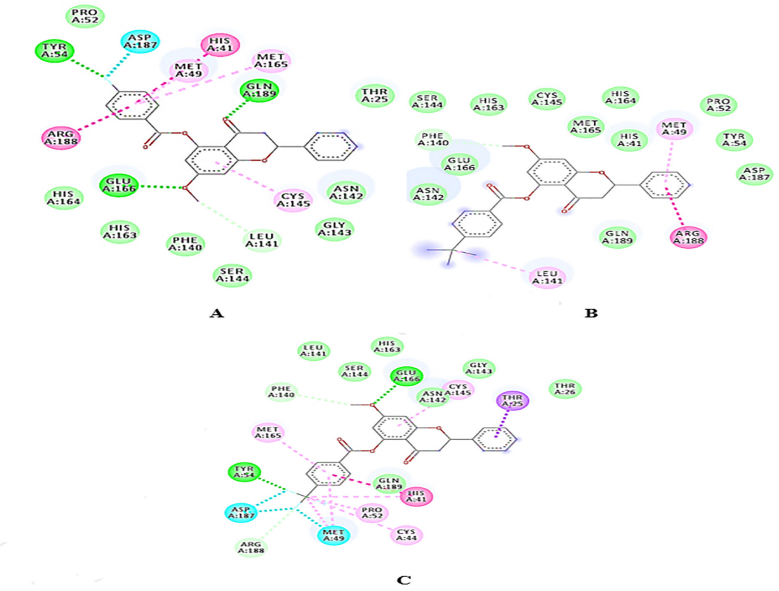

Figure 2. Interactions of (A) 4-fluoro-5-O-benzoylpinostrobin, (B) 4-t-butyl-5-O-benzoylpinostrobin, and (C) 4-trifluoromethyl-5-O-benzoylpinostrobin in amino acid residues from 5R84 receptors

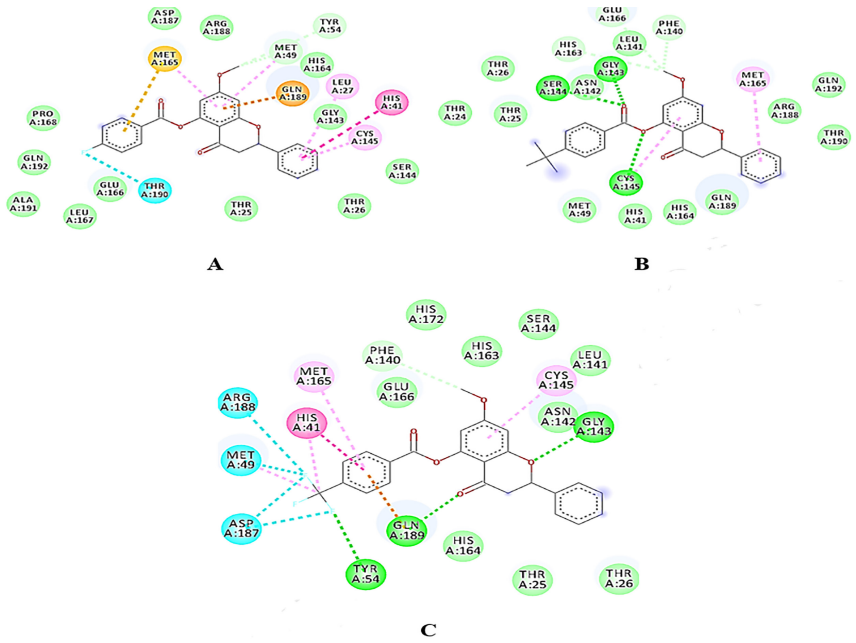

Figure 3. IInteractions of (A) 4-fluoro-5-O-benzoylpinostrobin, (B) 4-t-butyl-5-O-benzoylpinostrobin, and (C) 4-trifluoromethyl-5-O-benzoylpinostrobin in amino acid residues from 6LU7 receptors

is also relatively high, especially in the case of remdesivir. Indeed, the complex of nelfinavir-receptor (5R84) has the highest % similarity, but in the 6LU7 receptor, the ΔG value of nelfinavir is higher than the co-crystal ligand. In contrast, three reference ligands consisting of chloroquine, hydroxychloroquine, and favipiravir consistently rank last for the ΔG values in both receptors, even compared to all test ligands.

To facilitate the comparison of ΔG values and the % similarity of all test and reference ligands on the two receptors, a scatter diagram was made as presented in Figure 4. The diagram compares the difference in ΔG value between test and reference ligands and the co-crystal ligand with the % similarity of ligand-receptor interaction, where the line 0 on the x-axis indicates the position of the co-crystal ligand at each receptor. The area to the left of the 0 line shows a negative value, which means that the ΔG value of the ligand is lower than the co-crystal ligand, and vice versa. While on the y-axis, it shows the % similarity of ligand-receptor interaction compared to co-crystal ligand at each receptor. The more to the left and the higher the position of a ligand in the diagram, the stronger the prediction that the ligand has potential as an inhibitor at both receptors.

Table 5. Results of the docking of all reference ligands at the binding site of 5R84 receptor

Ligand	CQ	HCQ	FVP	IND	LPN	NFN	RMD
ΔG (kcal/mol)	-5.86 ± 0.05	-6.14 ± 0.09	-5.20 ± 0.00	-7.44 ± 0.05	-7.04 ± 0.09	-6.96 ± 0.13	-7.36 ± 0.17
Amino acid residues	-	25-Thr[a]	-	25-Thr[a]	25-Thr[a]	25-Thr[a]	25-Thr[a]
	-	26-Thr[a]	-	26-Thr[a]	26-Thr[a]	-	26-Thr[a]
	-	27-Leu[a]	-	-	27-Leu[a]	27-Leu[a]	27-Leu[a]
	41-His[a]	41-His[d]	41-His[c]	41-His[d]	41-His[d]	41-His[c]	41-His[i]
	44-Cys[a]	44-Cys[b]	-	-	-	-	-
	-	-	-	46-Ser[c]	-	46-Ser[a]	-
	49-Met[c]	49-Met[b]	49-Met[f]	49-Met[b]	49-Met[b]	49-Metg	49-Met[g]
	52-Pro[a]	52-Pro[b]	-	52-Pro[a]	52-Pro[a]	-	-
	54-Tyr[a]	54-Tyr[a]	-	54-Tyr[a]	54-Tyr[a]	54-Tyra	-
	-	-	-	-	-	140-Phea	-
	141-Leu[a]	-	-	-	-	141-Leua	-
	142-Asn[a]	142-Asn[a]	-	142-Asn[c]	142-Asn[c]	142-Asnc	142-Asn[a]
	-	143-Gly[a]	-	143-Gly[a]	143-Gly[a]	143-Glya	143-Gly[c]
	-	-	-	-	-	144-Sera	144-Ser[a]
	-	145-Cys[a]	-	145-Cys[c]	145-Cys[b]	145-Cysb	145-Cys[a]
	-	163-His[a]	-	-	-	163-His[a]	-
	164-His[a]	164-His[a]	164-His[a]	164-His[a]	164-His[a]	164-His[a]	164-His[a]
	165-Met[a]	165-Met[a]	165-Met[b]	165-Met[b]	165-Met[b]	165-Met[a]	165-Met[c]
	166-Glu[c]	166-Glu[a]	166-Glu[c]	166-Glu[c]	166-Glu[a]	166-Glu[a]	166-Glu[c]
	-	-	-	167-Leu[a]	-	-	167-Leu[a]
	-	-	-	168-Pro[a]	168-Pro[a]	-	168-Pro[a]
	187-Asp[a]	187-Asp[a]	-	187-Asp[a]	187-Asp[d]	187-Asp[a]	187-Asp[a]
	188-Arg[a]	188-Arg[c]	188-Arg[c]	188-Arg[d]	188-Arg[a]	188-Arg[a]	188-Arg[a]
	189-Gln[a]	189-Gln[a]	189-Gln[a]	189-Gln[a]	189-Gln[h]	189-Gln[a]	189-Gln[a]
	-	-	-	-	-	-	190-Thr[c]
	-	-	-	-	-	-	191-Ala[a]
	-	-	-	-	-	-	192-Gln[a]
The similarity of amino acids with co-crystal ligand (%)	71.43	78.57	50	71.43	85.71	100	78.57
The similarity in the type of interaction with co-crystal ligand (%)	35.71	42.86	14.29	28.57	42.86	50	42.86
The similarity of ligand-receptor interaction* (%)	25.51	33.67	7.14	20.41	36.73	50	33.67

[a]Van der Waals interaction; [b]Alkyl/Pi-alkyl interaction; [c]Hydrogen bond; [d]Pi-Pi T-shaped/Pi-Pi Stacked/Amide-Pi stacked; [e]Pi-sigma interaction; [f]Halogen; [g]Pi-Sulfur; [h]Unfavorable Bump/Donor-donor; [i]Pi-Cation/Anion; *Similarity of amino acids x similarity in type of interaction

Table 6. Results of the docking of all reference ligands at the binding site of 6LU7 receptor

Ligand	CQ	HCQ	FVP	IND	LPN	NFN	RMD
ΔG (kcal/mol)	-5.84 ± 0.11	-6.26 ± 0.09	-5.00 ± 0.07	-8.28 ± 0.04	-7.32 ± 0.11	-7.78 ± 0.11	-8.38 ± 0.08
Amino acid residues	-	-	-	24-Thr[c]	-	-	24-Thr[a]
	-	-	-	25-Thr[a]	25-Thr[a]	-	25-Thr[a]
	-	-	-	26-Thr[a]	26-Thr[a]	-	26-Thr[a]
	-	-	-	-	27-Leu[b]	-	27-Leu[a]
	-	-	40-Arg[a]	-	-	-	-
	41-His[a]	-	-	41-His[e]	41-His[c]	41-His[e]	41-His[c]
	-	-	-	-	-	-	45-Thr[a]
	-	-	-	-	46-Ser[a]	-	-
	49-Met[a]	-	-	49-Met[a]	49-Met[b]	49-Met[a]	49-Met[b]
	-	-	51-Asn[c]	-	-	-	-
	-	-	52-Pro[c]	-	-	-	-
	-	-	53-Asn[c]	-	-	-	-
	54-Tyr[a]	54-Tyr[a]	54-Tyr[a]	-	-	54-Tyr[a]	-
	-	-	55-Glu[c]	-	-	-	-
	140-Phe[a]	140-Phe[a]	-	140-Phe[a]	140-Phe[c]	140-Phe[a]	140-Phe[a]
	141-Leu[a]	141-Leu[c]	-	141-Leu[a]	141-Leu[a]	141-Leu[a]	141-Leu[a]
	142-Asn[a]	142-Asn[a]	-	142-Asn[a]	142-Asn[a]	142-Asn[a]	142-Asn[a]
	-	143-Gly[a]	-	143-Gly[a]	143-Gly[a]	-	143-Gly[c]
	144-Ser[a]	144-Ser[c]	-	144-Ser[a]	144-Ser[a]	144-Ser[a]	144-Ser[a]
	-	145-Cys[a]	-	145-Cys[c]	145-Cys[b]	145-Cys[a]	145-Cys[a]
	163-His[a]	163-His[a]	-	163-His[a]	-	163-His[b]	163-His[c]
	164-His[c]	164-His[a]	-	164-His[a]	164-His[a]	164-His[c]	164-His[a]
	165-Met[a]	165-Met[a]	-	165-Met[b]	165-Met[f]	165-Met[a]	165-Met[f]
	166-Glu[h]	166-Glu[a]	-	166-Glu[h]	166-Glu[c]	166-Glu[a]	166-Glu[c]
	-	-	-	167-Leu[a]	-	167-Leu[a]	-
	-	168-Pro[a]	-	168-Pro[a]	-	168-Pro[b]	168-Pro[a]
	-	-	-	-	-	170-Gly[a]	-
	-	172-His[a]	-	-	172-His[a]	172-His[a]	172-His[a]
	-	-	-	-	-	181-Phe[a]	-
	187-Asp[a]	-	-	187-Asp[a]	-	187-Asp[a]	187-Asp[a]
	188-Arg[a]	188-Arg[c]	188-Arg[c]	188-Arg[a]	188-Arg[a]	188-Arg[a]	188-Arg[a]
	189-Gln[a]	189-Gln[a]	-	189-Gln[c]	189-Gln[a]	189-Gln[g]	189-Gln[c]
	-	190-Thr[c]	-	190-Thr[a]	190-Thr[a]	190-Thr[d]	-
	-	191-Ala[a]	-	-	-	191-Ala[b]	-
	-	192-Gln[a]	-	192-Gln[a]	192-Gln[a]	-	-
The similarity of amino acids with co-crystal ligand (%)	78.57	50	71.43	85.71	100	78.57	
The similarity in the type of interaction with co-crystal ligand (%)	42.86	14.29	28.57	42.86	50	42.86	
The similarity of ligand-receptor interaction* (%)	33.67	7.14	20.41	36.73	50	33.67	

[a]Van der Waals interaction; [b]Alkyl/Pi-alkyl interaction; [c]Hydrogen bond; [d]Pi-Pi T-shaped/Pi-Pi Stacked/Amide-Pi stacked; [e]Pi-sigma interaction; [f]Pi-Sulfur; [g]Unfavorable Bump/Donor-donor; [h]Pi-Cation/Anion; *Similarity of amino acids x similarity in type of interaction

In Figure 4, it appears that for the 5R84 receptor (red), all test ligands and most of the reference ligands are in the left area of the diagram. As for the 6LU7 receptor (blue), only a few tests and reference ligands are in the left area of the diagram. The diagram shows that 4-fluoro-5-O-benzoylpinostrobin, 4-t-butyl-5-O-benzoylpinostrobin, and 4-trifluoromethyl-5-O-benzoylpinostrobin are predominantly in the upper left area of the diagram for each the receptor series, confirms the prediction that all three have the best potential as SARS-CoV-2 M^{Pro} inhibitors.

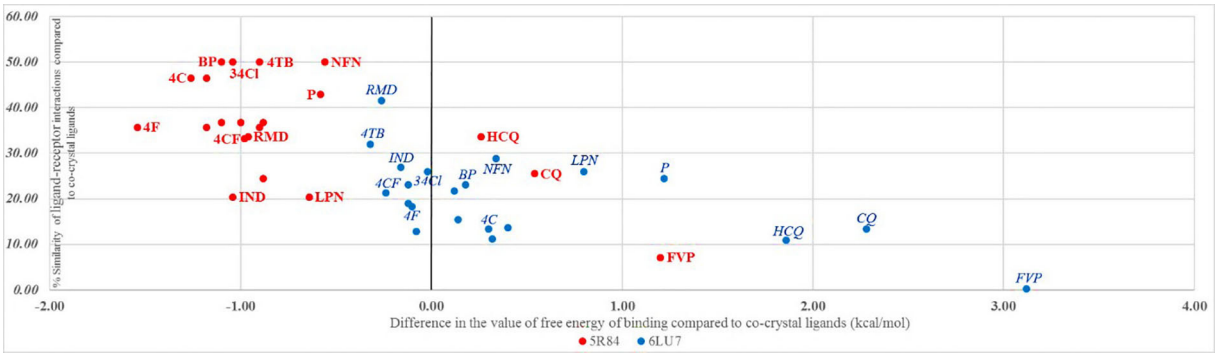

Figure 4. Diagram of the relationship between the difference in the value of free energy of binding and the percentage of similarity of ligand-receptor interactions compared to co-crystal ligands on the 5R84 (red) and 6LU7 (blue) receptors

Discussion

The docking protocol is done by using energy range 3, exhaustiveness 8, and the number of modes 9, which are the default values in the docking protocol using the Autodock Vina. Molecular docking was performed using configuration settings similar to the validation process, with changes to the test ligand file used.[41] However, it should be considered that the size of the grid box must be able to contain all the co-crystal ligands.[27] As for test and reference ligands, the grid box size does not have to be adjusted to the size of each ligand, because if it is too large each ligand will automatically adjust its position so that only the most active part of the ligand with the smallest ΔG is in the grid box.[36,42]

The docking process with Autodock Vina has advantages in terms of speed, accuracy and precision, where repetition from the docking process often results in ΔG values that are not significantly difference among individual runs.[30,43] However, unlike some other docking software such as Autodock 4 and MOE, the ΔG value of Autodock Vina only has an accuracy of 0.1 kcal/mol. Therefore, the accuracy of the docking results with Autodock Vina is often improved by repeating it several times to obtain an average ΔG value and its deviation which can have accuracy up to 0.01 kcal/mol depending on the number of repetitions.[44] It should be remembered that the results of the replication process depend on the condition of the hardware used, such as the amount of software that is run simultaneously to the stability of the voltage during the docking process. For this reason, it is important to set acceptable limits of deviation from the replication process, so that outlier values that can affect the average ΔG value can be excluded.[45] For this docking process, a limit for the deviation value of 0.2 kcal/mol is determined, with the consideration that repetition is carried out five times to obtain a more definite ΔG value. The value of RMSD is quite varied, which is quite low at the 5R84 receptor but almost exceeds the standard limit of 2 Å at the 6LU7 receptor. The high value of RMSD at 6LU7 receptors is due to the large size of the co-crystal ligand because it is a peptide-like molecule (PLM) consisting of six amino acids.[46] Besides, PLM is also known to have high enough molecular torque to allow variations in bond positions at the receptor-binding site. Calligari et al also reported that the 6LU7 receptor is less ideal for the docking process because it shows a closed binding pocket around the inhibitor, which may limit the effectiveness of the pose searching methods.[47] Therefore, two receptors are used as a comparison where the 5R84 receptor shows the binding pocket which is more ideal for the docking process.[22]

Analysis of amino acid residues from the redocking results as shown in Table 2 shows that the interaction between co-crystal ligands and binding sites on the 5R84 receptor is more influenced by weak bonds such as van der Waals interactions, whereas the 6LU7 receptor is involved in relatively many stronger interactions such as hydrogen bonds. Hydrophobic interactions in the form of alkyl/Pi-alkyl are more observed at 6LU7 receptors, where the hydrophobic interactions play a very important role in protease drug recognition.[47-49] It seems that the lower ΔG of co-crystal ligand at the 6LU7 receptor in comparison with 5R84 receptor is due to the presence of hydrophobic interactions and hydrogen bonds.

The docking results in Tables 3 to 6 show that all test and reference ligands give a lower ΔG value at the 5R84 receptor compared to 6LU7. However, this cannot justify that the 5R84 receptor is more precise than 6LU7 in docking to SARS-CoV-2 M^{Pro}. These results merely prove that receptors with broader binding sites most likelyto be closed tend to give a higher ΔG value than smaller, open-pocket binding sites receptors.[50] Theoretically, because the 5R84 and 6LU7 receptors are the same protein with similar amino acids, the results obtained should also be the same. However, the results from molecular docking do not produce dynamic ligand-receptor behavior as obtained from the results of molecular dynamics (MD) simulations. Therefore, it is important to conduct MD simulations for further analyses.

Interesting results were shown for three ligands with the lowest average ΔG in both receptors: 4-fluoro-5-O-benzoylpinostrobin, 4-t-butyl-5-O-benzoylpinostrobin, and 4-trifluoromethyl-5-O-benzoylpinostrobin. Besides having the lowest ΔG value compared to other test ligands, they also have similar types of interactions t to the pocket binding site,[47] including many halogen bonds in 4-fluoro-5-O-benzoylpinostrobin and 4-trifluoromethyl-5-O-benzoylpinostrobin as well as most hydrogen bonds on 4-t-butyl-5-O-benzoylpinostrobin. The advantage of this type of interaction can be particularly clearly observed

at 6LU7 receptor, where the ΔG values of these three ligands differ only slightly from those shown by remdesivir and indinavir as reference ligands. The 5R84 receptor is the opposite, where the three types of interactions are dominated by weak interactions in the form of van der Waals interactions, although both ligands with fluoro atoms still show halogen bonds. This indicate that the relationship between the ΔG value and the type of interactions can be more correlated at the 6LU7 receptor compared to the 5R84 receptor. That might be one of the reasons why the most docking research on SARS-CoV-2 M^{Pro} was done using 6LU7 receptors, as reported in several previous studies.[47,51-55]

The comparison of ΔG values and % similarity of the three ligands at each receptor is unique. Among the three, 4-fluoro-5-O-benzoylpinostrobin with Hansch parameters of hydrophobic (π) (+) and electronic (σ) (+) had the lowest ΔG and medium % similarity at 5R84, but the highest ΔG and the lowest % similarity at 6LU7. Furthermore, 4-t-butyl-5-O-benzoylpinostrobin with π (++++) but σ (-) has the highest ΔG and the highest % similarity at 5R84, also the lowest ΔG and the highest % similarity at 6LU7. Meanwhile, 4-trifluoromethyl-5-O-benzoylpinostrobin which possessed characteristics in the middle both with π (+++) and σ (+++) had medium ΔG and the lowest % similarity at 5R84 as well as medium ΔG and % similarity at 6LU7. However, it is difficult to draw a direct relationship between the value of ΔG and % similarity with the two parameters of Hansch. Apart from the data obtained that are still predictive in nature, there are other factors besides the chemical-physical parameters that determine the biological activity of a compound.[56] The most rational way to draw relationship can be conducted by direct testof these compounds with variations in the properties of chemical-physical parameters and then formulate them in the QSAR equation with the most influential descriptors,[57] which is the focused to be continued from this research.

Interesting results are also shown in the reference ligand used, where in general the results obtained can be divided into three categories. First, ligands with low ΔG values in both receptors as indicated by remdesivir and indinavir. The results in this group seemed to be convincing that both ligands did have potential as SARS-CoV-2 M^{Pro} inhibitors. Several previous studies also reported that remdesivir had a fairly low ΔG value against SARS-CoV-2 M^{Pro},[17,24] although the other study reported that remdesivir also had activity against SARS-CoV-2 RdRp.[58] These results are in line with previous preclinical studies which state that remdesivir has the potential to inhibit viral infection at low-micromolar concentration and showed high SI.[59-62] Not surprisingly, currently remdesivir has been authorized by the FDA for COVID-19 treatment, even for emergencies.[63] As for indinavir, although the testing was not as extensive as remdesivir, it also showed good signs of having the potential to treat COVID-19.[64]

Second, ligands with low ΔG values at the 5R84 receptor but high enough at the 6LU7 receptor, as shown by lopinavir and nelfinavir. These results indicate that these compounds may have potential as SARS-CoV-2 M^{Pro} inhibitors under certain conditions but may have other targets for COVID-19 receptors such as ACE2 and RdRp.[65] One of them was reported by Eton et al. which mentioned indinavir has potential as a SARS-CoV-2 M^{Pro} inhibitor,[20] whereas in other studies Xu et al. also reported similar results by nelfinavir.[66] However, both tests are still in the virtual screening stage and still need to be proven experimentally in the laboratory, including the possibility of other potential targets besides SARS-CoV-2 M^{Pro}.[67]

Finally, ligands with high ΔG values in both receptors, exemplified by chloroquine, hydroxychloroquine, and favipiravir. These results are very interesting, especially because of promising results in COVID-19 therapy in various studies. Chloroquine and hydroxychloroquine are reported to show satisfactory results in various in vitro studies for limiting the replication of SARS-CoV-2,[7,68,69] while favipiravir shows good therapeutic response on COVID-19 in terms of disease progression and viral clearance.[70] These therapeutic agentshave different target receptors, where chloroquine and hydroxychloroquine are reported to have acted as ACE2 inhibitors,[7,71] while favipiravir shows potential as an RdRp inhibitor.[72] The results of this study also suggested that the target of the three proposed compounds (i.e. 4-fluoro-5-O-benzoylpinostrobin, 4-t-butyl-5-O-benzoylpinostrobin, and 4-trifluoromethyl-5-O-benzoylpinostrobin) is most likely not SARS-CoV-2 M^{Pro}, but all three molecules still have the potential as COVID-19 drugs through other mechanisms of action besides SARS-CoV-2 M^{Pro} inhibitors.

Conclusion

In conclusion, this study opens the opportunity for new compounds that have the potential to be developed in COVID-19 therapy as a SARS-CoV-2 M^{Pro} inhibitor. The enormous potential is mainly shown by three ligands consisting of 4-fluoro-5-O-benzoylpinostrobin, 4-t-butyl-5-O-benzoylpinostrobin, and 4-trifluoromethyl-5-O-benzoylpinostrobin, which shows the lowest ΔG of both receptors SARS-CoV-2 M^{Pro} used. All three ligands have even better potential than co-crystal ligands and reference compounds such as remdesivir which is currently in clinical trials. The current *in silico* investigation is a preliminary work which necessitates future preclinical and clinical studies for verification of the results and expected to be the first step in development of 5-O-benzoylpinostrobin derivatives in COVID-19 therapy.

Acknowledgments

This research was funded by an internal grant from Universitas Airlangga. The authors are thankful to the Department of Pharmaceutical Science, Faculty of Pharmacy, Universitas Airlangga, for providing the necessary facilities and infrastructure to carry out the project.

Conflict of Interest

The authors claim that there is no conflict of interest.

References

1. Zheng J. SARS-CoV-2: an Emerging Coronavirus that Causes a Global Threat. Int J Biol Sci. 2020;16(10):1678-85. doi:10.7150/ijbs.45053
2. Rudan I. A cascade of causes that led to the COVID-19 tragedy in Italy and in other European Union countries. J Glob Health. 2020;10(1):010335. doi:10.7189/jogh-10-010335
3. Biswas A, Bhattacharjee U, Chakrabarti AK, Tewari DN, Banu H, Dutta S. Emergence of Novel Coronavirus and COVID-19: whether to stay or die out? Crit Rev Microbiol. 2020;46(2):182-193. doi:10.1080/1040841X.2020.1739001
4. Talevi A, Bellera CL. Challenges and opportunities with drug repurposing: finding strategies to find alternative uses of therapeutics. Expert Opin Drug Discov. 2020;15(4):397-401. doi:10.1080/17460441.2020.1704729
5. Wang Y, Zhang D, Du G, Du R, Zhao J, Jin Y, et al. Remdesivir in adults with severe COVID-19: a randomised, double-blind, placebo-controlled, multicentre trial. Lancet. 2020;395(10236):1569-78. doi:10.1016/S0140-6736(20)31022-9
6. Norrie JD. Remdesivir for COVID-19: challenges of underpowered studies. Lancet. 2020;395(10236):1525-27. doi:10.1016/S0140-6736(20)31023-0
7. Devaux CA, Rolain JM, Colson P, Raoult D. New insights on the antiviral effects of chloroquine against coronavirus: what to expect for COVID-19? Int J Antimicrob Agents. 2020;55(5):105938. doi:10.1016/j.ijantimicag.2020.105938
8. Tu YF, Chien CS, Yarmishyn AA, Lin YY, Luo YH, Lin YT, et al. A review of SARS-CoV-2 and the ongoing clinical trials. Int J Mol Sci. 2020;21(7):2657. doi:10.3390/ijms21072657
9. Cava C, Bertoli G, Castiglioni I. *In silico* discovery of candidate drugs against covid-19. Viruses. 2020;12(4):404. doi:10.3390/v12040404
10. 10. Ciliberto G, Cardone L. Boosting the arsenal against COVID-19 through computational drug repurposing. Drug Discov Today. 2020;25(6):946-48. doi:10.1016/j.drudis.2020.04.005
11. Liu C, Zhou Q, Li Y, Garner LV, Watkins SP, Carter LJ, et al. Research and development on therapeutic sgents and vaccines for COVID-19 and related human coronavirus diseases. ACS Cent Sci. 2020;6(3):315-31. doi:10.1021/acscentsci.0c00272
12. 12. Sanders JM, Monogue ML, Jodlowski TZ, Cutrell JB. Pharmacologic treatments for coronavirus disease 2019 (COVID-19). JAMA. 2020;323(18):1824-36. doi:10.1001/jama.2020.6019
13. Redeploying plant defences. Nat Plants. 2020;6(3):177. doi:10.1038/s41477-020-0628-0
14. Zhang D, Wu K, Zhang X, Deng S, Peng B. *In silico* screening of Chinese herbal medicines with the potential to directly inhibit 2019 novel coronavirus. J Integr Med. 2020;18(2):152-8. doi:10.1016/j.joim.2020.02.005
15. Yi Y, Lagniton PNP, Ye S, Li E, Xu RH. COVID-19: what has been learned and to be learned about the novel coronavirus disease. Int J Biol Sci. 2020;16(10):1753-66. doi:10.7150/ijbs.45134
16. Lu H. Drug treatment options for the 2019-new coronavirus (2019-nCoV). Biosci Trends. 2020;14(1):69-71. doi:10.5582/bst.2020.01020
17. Enmozhi SK, Raja K, Sebastine I, Joseph J. Andrographolide as a potential inhibitor of SARS-CoV-2 main protease: an *in silico* approach. J Biomol Struct Dyn. 2020. doi:10.1080/07391102.2020.1760136
18. Zhang L, Lin D, Sun X, Curth U, Drosten C, Sauerhering L, et al. Crystal structure of SARS-CoV-2 main protease provides a basis for design of improved α-ketoamide inhibitors. Science. 2020;368(6489):409-12. doi:10.1126/science.abb3405
19. Astuti I, Ysrafil. Severe Acute Respiratory Syndrome Coronavirus 2 (SARS-CoV-2): An overview of viral structure and host response. Diabetes Metab Syndr. 2020;14(4):407-12. doi:10.1016/j.dsx.2020.04.020
20. Ton AT, Gentile F, Hsing M, Ban F, Cherkasov A. Rapid identification of potential inhibitors of SARS-CoV-2 main protease by deep docking of 1.3 billion compounds. Mol Inform. 2020. doi:10.1002/minf.202000028
21. Jin Z, Du X, Xu Y, Deng Y, Liu M, Zhao Y, et al. Structure of Mpro from COVID-19 virus and discovery of its inhibitors. Nature. 2020;582(7811):289-93. doi:10.1038/s41586-020-2223-y
22. Boopathi S, Poma AB, Kolandaivel P. Novel 2019 coronavirus structure, mechanism of action, antiviral drug promises and rule out against its treatment. J Biomol Struct Dyn. 2020. doi:10.1080/07391102.2020.1758788
23. Rathinavel T, Palanisamy M, Palanisamy S, Subramanian A, Thangaswamy S. Phytochemical 6-gingerol – A promising drug of choice for COVID-19. Int J Adv Sci Eng.2020;6(4):1482-9. doi:10.29294/IJASE.6.4.2020.1482-1489
24. Wu C, Liu Y, Yang Y, Zhang P, Zhong W, Wang Y, et al. Analysis of therapeutic targets for SARS-CoV-2 and discovery of potential drugs by computational methods. Acta Pharm Sin B. 2020;10(5):766-88. doi:10.1016/j.apsb.2020.02.008
25. Chahyadi A, Hartati R, Wirasutisna KR, Elfahmi. *Boesenbergia pandurata* Roxb., an indonesian medicinal plant: phytochemistry, biological activity, plant biotechnology. Procedia Chem. 2014;13:13-37. doi:10.1016/j.proche.2014.12.003
26. Tewtrakul S, Subhadhirasakul S, Puripattanavong J, Panphadung T. HIV-1 protease inhibitory substances from the rhizomes of *Boesenbergia pandurata* Holtt.

Songklanakarin J Sci Technol. 2003;25(4):503-8.
27. Pratama MRF, Poerwono H, Siswandono S. Design and molecular docking of novel 5-O-benzoylpinostrobin derivatives as anti-breast cancer. Thai J Pharm Sci. 2019;43(4):201-12.
28. Pratama MRF, Poerwono H, Siswodihardjo S. Molecular docking of novel 5-O-benzoylpinostrobin derivatives as wild type and L858R/T790M/V948R mutant EGFR inhibitor. J Basic Clin Physiol Pharmacol. 2019;30(6):20190301. doi:10.1515/jbcpp-2019-0301
29. Pratama MRF, Poerwono H, Siswodiharjo S. ADMET properties of novel 5-O-benzoylpinostrobin derivatives. J Basic Clin Physiol Pharmacol. 2019;30(6):20190251. doi:10.1515/jbcpp-2019-0251
30. Trott O, Olson AJ. AutoDock Vina: improving the speed and accuracy of docking with a new scoring function, efficient optimization and multithreading. J Comput Chem. 2010;31(2):455-61. doi:10.1002/jcc.21334
31. O'Boyle NM, Banck M, James CA, Vandermeersch T, Hutchison GR. Open Babel: An open chemical toolbox. J Cheminformatics. 2011;3:33. doi:10.1186/1758-2946-3-33
32. Yuan S, Chan S, Hu Z. Using PyMOL as a platform for computational drug design. Wiley Interdiscip Rev Comput Mol Sci. 2017;7(2):1298. doi:10.1002/wcms.1298
33. Pettersen EF, Goddard TD, Huang CC, Couch GS, Greenblatt DM, Meng EC, et al. UCSF Chimera--a visualization system for exploratory research and analysis. J Comput Chem. 2004;25(13):1605-12. doi:10.1002/jcc.20084
34. Forli S. Charting a Path to Success in Virtual Screening. Molecules. 2015;20(10):18732-58. doi:10.3390/molecules201018732
35. Elokely KM, Doerksen RJ. Docking challenge: Protein sampling and molecular docking performance. J Chem Inf Model. 2013;53(8):1934-45. doi:10.1021/ci400040d
36. 36. Ramirez D, Caballero J. Is It reliable to take the molecular docking top scoring position as the best solution without considering available structural data? Molecules. 2018;23(5):1038. doi:10.3390/molecules23051038
37. Feinstein WP, Brylinski M. Calculating an optimal box size for ligand docking and virtual screening against experimental and predicted binding pockets. J Cheminform. 2015;7:18. doi:10.1186/s13321-015-0067-5
38. Macari G, Toti D, Moro CD, Polticelli F. Fragment-based ligand-protein contact statistics: application to docking simulations. Int J Mol Sci. 2019;20(10):2499. doi:10.3390/ijms20102499
39. Forli S, Huey R, Pique ME, Sanner M, Goodsell DS, Olson AJ. Computational protein-ligand docking and virtual drug screening with the AutoDock suite. Nat Protoc. 2016;11:905-19. doi:10.1038/nprot.2016.051
40. Ding Y, Fang Y, Moreno J, Ramanujam J, Jarrell M, Brylinski M. Assessing the similarity of ligand binding conformations with the Contact Mode Score. Comput Biol Chem. 2016;64:403-13. doi:10.1016/j.compbiolchem.2016.08.007
41. Ferreira LG, Dos Santos RN, Oliva G, Andricopulo AD. Molecular docking and structure-based drug design strategies. Molecules. 2015;20(7):13384-421. doi:10.3390/molecules200713384
42. Mortier J, Dhakal P, Volkamer A. Truly target-focused pharmacophore modeling: a novel tool for mapping intermolecular surfaces. Molecules. 2018;23(8):1959. doi:10.3390/molecules23081959
43. Nguyen NT, Nguyen TH, Pham TNH, Huy NT, Bay MV, Pham MQ, et al. Autodock vina adopts more accurate binding poses but autodock4 forms better binding sffinity. J Chem Inf Model. 2020;60(1):204-11. doi:10.1021/acs.jcim.9b00778
44. Castro-Alvarez A, Costa AM, Vilarrasa J. The Performance of several docking programs at reproducing protein–macrolide-like crystal structures. Molecules. 2017;22(1):136. doi:10.3390/molecules22010136
45. Sliwoski G, Kothiwale S, Meiler J, Lowe EW. Computational methods in drug discovery. Pharmacol Rev. 2014;66(1):334-95. doi:10.1124/pr.112.007336
46. Pant S, Singh M, Ravichandiran V, Murty USN, Srivastava HK. Peptide-like and small-molecule inhibitors against Covid-19. J Biomol Struct Dyn. 2020. doi:10.1080/07391102.2020.1757510
47. Calligari P, Bobone S, Ricci G, Bocedi A. Molecular investigation of SARS-CoV-2 proteins and their interactions with antiviral drugs. Viruses. 2020;12(4):445. doi:10.3390/v12040445
48. Muramatsu T, Takemoto C, Kim YT, Wang H, Nishii W, Terada T, et al. SARS-CoV 3CL protease cleaves its C-terminal autoprocessing site by novel subsite cooperativity. Proc Natl Acad Sci U S A. 2016;113(46):12997-3002. doi:10.1073/pnas.1601327113
49. Patick AK, Potts KE. Protease inhibitors as antiviral agents. Clin Microbiol Rev. 1998;11(4):614-27.
50. Ma B, Shatsky M, Wolfson HJ, Nussinov R. Multiple diverse ligands binding at a single protein site: A matter of pre-existing populations. Protein Sci. 2002;11(2):184-97. doi:10.1110/ps.21302
51. Odhar HA, Ahjel SW, Albeer AAMA, Hashim AF, Rayshan AM, Humadi SS. Molecular docking and dynamics simulation of FDA approved drugs with the main protease from 2019 novel coronavirus. Bioinformation. 2020;16(3):236-44. doi:10.6026/97320630016236
52. Narkhede RR, Cheke RS, Ambhore JP, Shinde SD. The molecular docking study of potential drug candidates showing anti-COVID-19 activity by exploring of therapeutic targets of SARS-CoV-2. Eurasian J Med Oncol. 2020;4(3):185-95. doi:10.14744/

ejmo.2020.31503
53. Beck BR, Shin B, Choi Y, Park S, Kang K. Predicting commercially available antiviral drugs that may act on the novel coronavirus (SARS-CoV-2) through a drug-target interaction deep learning model. Comput Struct Biotechnol J. 2020;18:784-90. doi:10.1016/j.csbj.2020.03.025
54. Kumar D, Kumari K, Jayaraj A, Kumar V, Kumar RV, Dass SK, et al. Understanding the binding affinity of noscapines with protease of SARS-CoV-2 for COVID-19 using MD simulations at different temperatures. J Biomol Struct Dyn. 2020;[Epub ahead of print]. doi:10.1080/07391102.2020.1752310
55. Hall DC, Ji HF. A search for medications to treat COVID-19 via *in silico* molecular docking models of the SARS-CoV-2 spike glycoprotein and 3CL protease. Travel Med Infect Dis. 2020;35:101646. doi:10.1016/j.tmaid.2020.101646
56. Priyadarsini KI. Chemical and structural features influencing the biological activity of curcumin. Curr Pharm Des. 2013;19(11):2093-100. doi:10.2174/138161213805289228
57. Cherkasov A, Muratov EN, Fourches D, Varnek A, Baskin II, Cronin M. et al. QSAR modeling: where have you been? Where are you going to? J Med Chem. 2014;57(12):4977-5010. doi:10.1021/jm4004285
58. Chen YW, Yiu CPB, Wong KY. Prediction of the SARS-CoV-2 (2019-nCoV) 3C-like protease (3CL pro) structure: virtual screening reveals velpatasvir, ledipasvir, and other drug repurposing candidates. F1000Res. 2020;9:129. doi:10.12688/f1000research.22457.2
59. Wang M, Cao R, Zhang L, Yang X, Liu J, Xu M, et al. Remdesivir and chloroquine effectively inhibit the recently emerged novel coronavirus (2019-nCoV) in vitro. Cell Res. 2020;30:269-71. doi:10.1038/s41422-020-0282-0
60. Sheahan TP, Sims AC, Leist SR, Schafer A, Won J, Brown AJ, et al. Comparative therapeutic efficacy of remdesivir and combination lopinavir, ritonavir, and interferon beta against MERS-CoV. Nat Commun. 2020;11(1):222. doi:10.1038/s41467-019-13940-6
61. Yan Y, Shin WI, Pang YX, Meng Y, Lai J, You C. et al. The first 75 days of novel coronavirus (SARS-CoV-2) outbreak: recent advances, prevention, and treatment. Int J Environ Res Public Health. 2020;17(7):2323. doi:10.3390/ijerph17072323
62. Cao Y, Deng Q, Dai S. Remdesivir for severe acute respiratory syndrome coronavirus 2 causing COVID-19: An evaluation of the evidence. Travel Med Infect Dis. 2020;35:101647. doi:10.1016/j.tmaid.2020.101647
63. Remdesivir EUA Fact sheet for Patients and Parents and Caregivers. https://www.fda.gov/media/137565/download. Accessed 5 May 2020.
64. Contini A. Virtual screening of an FDA approved drugs database on two COVID-19 coronavirus proteins. ChemRxiv. 2020. doi:10.26434/chemrxiv.11847381.v1
65. Huang J, Song W, Huang H, Sun Q. Pharmacological therapeutics targeting RNA-dependent RNA polymerase, proteinase and spike protein: from mechanistic studies to clinical trials for COVID-19. J Clin Med. 2020;9(4):1131. doi:10.3390/jcm9041131
66. Xu Z, Peng C, Shi Y, Zhu Z, Mu K, Wang X, et al. Nelfinavir was predicted to be a potential inhibitor of 2019-nCov main protease by an integrative approach combining homology modelling, molecular docking and binding free energy calculation. BioRxiv. 2020. doi:10.1101/2020.01.27.921627
67. Rismanbaf A. Potential treatments for COVID-19; a narrative literature review. Arch Acad Emerg Med. 2020;8(1):29.
68. Principi N, Esposito S. Chloroquine or hydroxychloroquine for prophylaxis of COVID-19. Lancet Infect Dis. 2020;20(10):1118. doi:10.1016/S1473-3099(20)30296-6
69. 69. Cortegiani A, Ingoglia G, Ippolito M, Giarratano A, Einav S. A systematic review on the efficacy and safety of chloroquine for the treatment of COVID-19. J Crit Care. 2020;57:279-283. doi:10.1016/j.jcrc.2020.03.005
70. 70. Cai Q, Yang M, Liu D, Chen J, Shu D, Xia J, et al. Experimental treatment with favipiravir for COVID-19: An open-label control study. Engineering. 2020. doi:10.1016/j.eng.2020.03.007
71. Liu J, Cao R, Xu M, Wang X, Zhang H, Hu H, et al. Hydroxychloroquine, a less toxic derivative of chloroquine, is effective in inhibiting SARS-CoV-2 infection in vitro. Cell Discov. 2020;6:16. doi:10.1038/s41421-020-0156-0
72. Dong L, Hu S, Gao J. Discovering drugs to treat coronavirus disease 2019 (COVID-19). Drug Discov Ther. 2020;14(1):58-60. doi:10.5582/ddt.2020.01012